On the validity of hydrodynamics in plane Poiseuille flows

M. Malek Mansour [a,*], F. Baras [a], Alejandro L. Garcia [b,1]

[a] *Center for Nonlinear Phenomena and Complex Systems, Université Libre de Bruxelles, Campus Plaine, CP 231, Blvd. du Triomphe, B-1050 Brussels, Belgium*
[b] *Center for Computational Sciences and Engineering, Lawrence Berkeley National Laboratory, Berkeley, CA 94720, USA*

Abstract

Microscopic simulations of plane Poiseuille flow for a dilute gas are presented. Although the flow is laminar (Reynolds number ≈ 10) and sub-sonic, the temperature and pressure profiles measured in the simulations differ qualitatively from the hydrodynamic predictions. The results are in agreement with a recent theoretical analysis based on the asymptotic solution of the BGK model of the Boltzmann equation.

1. Introduction

One of the fundamental issues explored by molecular simulations, to which Bill Hoover has so greatly contributed, pertains to the limit of validity of phenomenological equations, such as the Navier–Stokes equations of hydrodynamics. For example, the presumption that collective fluid motion could occur only at macroscopic scales was overturned by the pioneering molecular dynamics experiments of Alder and Wainwright [1]. Extensions of this work demonstrated that an appropriate generalization of hydrodynamics describes fluid properties in the bulk correctly, even at molecular scales [2].

With the growing power of computers, a rich spectrum of *nonequilibrium* phenomena was found in particle simulations [3–5]. Hydrodynamic instabilities, such as vortex

---

* Corresponding author. E-mail: fbaras@ulb.ac.be.
[1] Permanent address: Department of Physics, San Jose State University, San Jose, CA 95192, USA.

shedding behind an obstacle [6] and Rayleigh–Bénard convection rolls [7,8], have been observed in systems containing only a few thousand atoms. The appearance of these hydrodynamic-like behavior naturally raises the question as to how accurately they are described by standard fluid dynamics. Up to now, studies have indicated that, except for certain extreme conditions (e.g., high Mach number shock waves [9]), the hydrodynamic equations remain surprisingly robust [10,11]. At microscopic scales, the most noticeable deviation from conventional fluid mechanics was found to be in the treatment of the boundaries. The standard macroscopic boundary conditions cannot be applied since the distribution of molecules approaching and leaving a surface do not combine to form a correct local equilibrium distribution. This effect was known to Maxwell [12] and his insightful predictions of velocity slip and temperature jump remain applicable today in a variety of situations. For example, in shear or Poiseuille flows, the velocity field predicted from the slip-corrected Navier–Stokes equations is in quantitative agreement with particle simulations [13]. The same conclusion holds for the temperature jump in a gas, subject to a constant temperature gradient [14] and in exothermic reactive fluids in contact with thermal reservoirs [15].

In view of these impressive results, one is led to inquire whether there exist simple flows for which the hydrodynamic equations give the wrong *qualitative* result, even when the microscopic boundary corrections are included. As we will show in this paper, the answer is in the affirmative.

The microscopic simulation of plane Poiseuille flow and the corresponding hydro-dynamic predictions are presented in Section 2. The BGK model of the Boltzmann equation and its perturbation expansion for this system are discussed in Section 3. It is shown that this expansion leads to predictions that are in qualitative agreement with the simulation results and that quantitative agreement is obtained by adjusting the transport properties to match the hard sphere values. Concluding remarks and perspectives are presented in Section 4.

2. Microscopic simulation of Poiseuille flow

Consider an assembly of N particles confined between two rigid parallel plates located at $Y = \pm L/2$. The plates are stationary and act as thermal reservoirs, that is, each time a particle strikes a plate it is re-injected into the system with its velocity randomly assigned from a half-Maxwellian distribution at the reservoir temperature T_R. Periodic boundary conditions are assumed in the other two directions and a constant acceleration field, a, oriented along the X-axis is applied to the system. Assuming the flow is laminar, the hydrodynamic equations lead to the stationary velocity profile [16],

$$\mathbf{u}(Y) = \frac{\rho a}{2\eta}[(L/2)^2 - Y^2]\mathbf{1}_x + u_{\text{slip}}\mathbf{1}_x \,, \tag{1}$$

where $\mathbf{1}_x$ is the unit vector in the X-direction, ρ and η are the mass density and shear viscosity, respectively, and u_{slip} is the velocity slip at the walls. For a dilute gas,

elementary kinetic theory gives [17,18]

$$u_{\text{slip}} = \frac{5\pi}{16} \lambda \left| \frac{\partial u}{\partial Y} \right|_{\text{wall}} , \tag{2}$$

where λ is the mean free path in the gas.

Because of energy dissipation from viscous heating, the system also develops a temperature profile. Elementary hydrodynamic calculation leads to

$$T(Y) = T_R + \frac{a^2 \rho^2}{12 \eta \kappa} [(L/2)^4 - Y^4] + T_{\text{jump}} , \tag{3}$$

where κ is the thermal conductivity and $T_{\text{jump}} \equiv T(Y = \pm L/2) - T_R$ is the temperature jump at the boundaries. For dilute gases, one has [18,19]

$$T_{\text{jump}} = \frac{m\kappa}{2\rho k_B} \sqrt{\frac{m\pi}{2k_B T}} \left| \frac{\partial T}{\partial Y} \right|_{\text{wall}} , \tag{4}$$

where m and k_B are the particle mass and Boltzmann's constant, respectively. Since the fluid velocity normal to the plates is strictly zero the pressure in the gas is constant.

For the microscopic simulations, we consider a fluid consisting of N hard spheres with diameter d at a number density of $n = 1.21 \times 10^{-3}$ particles per d^3, leading to a mean free path $\lambda = 186d$. This corresponds to a dilute gas, well within the validity of the Boltzmann equation and so we use Bird's direct simulation Monte Carlo (DSMC) algorithm [20] which is particularly well adapted for the simulation of Boltzmann gases. As a numerical method DSMC is several orders of magnitude faster than a corresponding molecular dynamics simulation of the exact hard-sphere dynamics. Each run evaluates about 10^6 collisions per particle; the statistical errors, estimated by dividing a run into 10 samples, is about 0.4% for the velocity and temperature profiles and less than 0.1% for the hydrostatic pressure profile.

The following convention will be used throughout the article: lengths and masses are scaled by the particle diameter d and mass m, respectively. The temperature is scaled by the reservoir temperature T_R and the velocities by the most probable thermal speed, $\sqrt{2k_B T/m}$. With these conventions, Boltzmann's constant $k_B = 0.5$ and the sound speed is about 0.913, in simulation units.

We first consider a system made up of $N = 1000$ hard spheres that is 10 mean free paths wide ($L = 1860d$) and choose an acceleration field $a = 1.6 \times 10^{-4}$. The maximum fluid velocity is then $u_{max} \approx 0.61$ and the Reynolds number is $Re \approx 10$ so the flow is sub-sonic and laminar. Fig. 1 represents the measured velocity profile together with its corresponding hydrodynamic expression (1), with the boundary slip (2) included. As the figure shows, the agreement is mainly qualitative, the relative deviation being around 10%. On the other hand, Fig. 2 shows that the measured temperature profile *qualitatively* contradicts the hydrodynamic result, as given by (3), since the profile is bimodal with a "dimple" in the center. Furthermore, the temperature jump at the boundaries is more than twice the value predicted by (4). Note that in Fig. 2 the temperature profile given by (3) has been shifted upward so as to match the measured
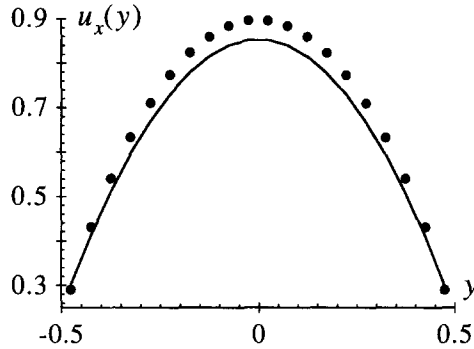
Fig. 1. Stationary velocity profile for a system that is 10 mean free paths wide; number density $n = 1.21 \times 10^{-3}$ and acceleration $a = 1.6 \times 10^{-4}$. The circles are simulation data and the solid line is from Eq. (1).
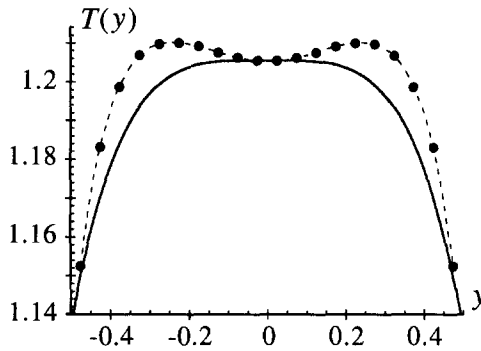

Fig. 2. Stationary temperature profile for a 10 mean free paths wide system; number density $n = 1.21 \times 10^{-3}$ and acceleration $a = 1.6 \times 10^{-4}$. The circles are simulation data and the solid line is from Eq. (3).

values at the middle of the system $Y = 0$; with this displacement the relative deviations are about 1%.

Although the relative temperature variations throughout the system remain small (less than 10%), a possible source of the observed discrepancy in the profiles is the state-dependence of the transport coefficients. In writing (1) and (3), we have assumed that both the mass density and transport coefficients are constant. For a hard-sphere Boltzmann gas, however, the mass density varies as the inverse of the temperature (at fixed pressure) and the transport coefficients are given by the Chapman–Enskog expressions,

$$\eta = \frac{5}{16d^2} \sqrt{\frac{mk_B T}{\pi}}; \qquad \kappa = \frac{15k_B}{4m} \eta. \tag{5}$$

Taking the above relations into account complicates the structure of the hydrodynamic equations but they can easily be solved numerically. The results remain quite close to
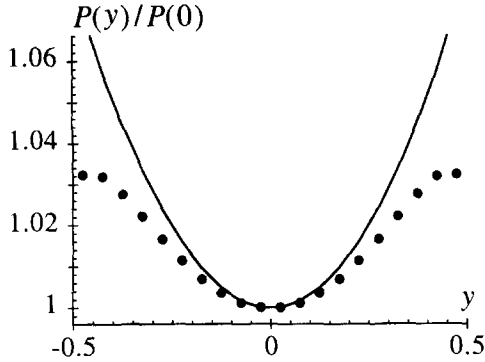
$P(y)/P(0)$

Fig. 3. Stationary pressure profile for a 10 mean free paths wide system; number density $n = 1.21 \times 10^{-3}$ and acceleration $a = 1.6 \times 10^{-4}$. The circles are simulation data and the solid line is the BGK first-order correction (see Eq. (18)). Both results are normalized by their corresponding values at the center of the system, $y = 0$.
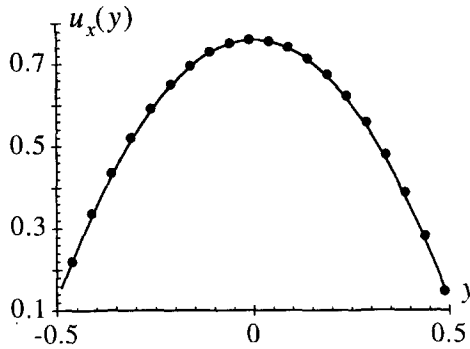
$u_x(y)$

Fig. 4. Stationary velocity profile for a system that is 20 mean free paths wide; number density $n = 1.21 \times 10^{-3}$ and acceleration $a = 4 \times 10^{-5}$. The circles are simulation data and the solid line is from Eq. (1).

those given by the simple formulae (1) and (3), except for the temperature jump (4) which shows a better agreement with the simulation result.

The profiles observed in the simulation, especially the temperature profile (Fig. 2), are quite surprising. Though the system is small $(L = 10\lambda)$, the average velocity and temperature variations, over a mean free path, do not exceed 1.5%, so one would legitimately expect the hydrodynamic description to remain valid. Yet the observed bimodal temperature profile is structurally different from the hydrodynamic prediction. This discrepancy is further illustrated by the hydrostatic pressure profile shown in Fig. 3. According to hydrodynamics the pressure should be constant across the channel, even if the temperature-dependence of the mass density and transport coefficients is taken into account. Fig. 3 clearly indicates that it is not the case.
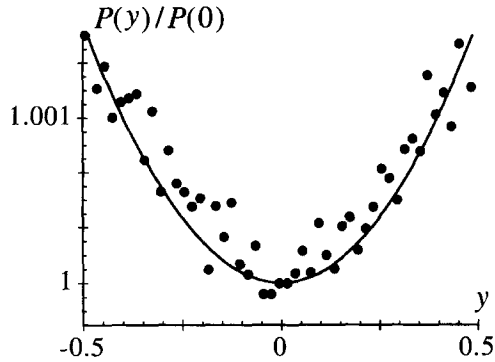
Fig. 5. Stationary pressure profile for a 100 mean free paths wide system; number density $n = 1.21 \times 10^{-3}$ and acceleration $a = 1.6 \times 10^{-6}$. The circles are simulation data and the solid line is the BGK first-order correction (see Eq. (18)). Both results are normalized by their corresponding values at the center of the system, $y = 0$.

To identify the origin of these discrepancies, we have considered several different simulations, including a dense Lennard–Jones fluid [21]. The key parameter turns out to be the Knudsen number, $Kn \equiv \lambda/L$. When the Knudsen number is lowered, either by increasing the number density or the system width, the discrepancy gradually disappears. For instance, a quantitative agreement for the velocity profile is observed already when the distance between the plates is increased to twenty mean free paths (see Fig. 4). On the other hand, the qualitative discrepancy with the pressure profile persists even for systems as wide as $L = 100\lambda$ (see Fig. 5).

3. Beyond hydrodynamics

The validity of the hydrodynamic description of a fluid rests on two fundamental hypotheses. First, the local equilibrium assumption which stipulates that within each fluid volume element the equilibrium equation of state remains valid, even though the system is globally out of equilibrium. Second, the linear response assumption which requires that fluxes obey transport laws that are linear in the gradients of velocity and temperature (i.e., the Newton and Fourier laws). Both assumptions are expected to break down when gradients are very large, as for example in a high Mach number shock wave [9,20]. In any case, the Knudsen number must remain small since otherwise there may not be enough collisions to restore the local Maxwellian distribution, thus compromising the local equilibrium assumption. For example, within a mean free path of a boundary the distribution of particles approaching and leaving that boundary do not combine to form the correct local equilibrium distribution.

The results of our simulations clearly indicate the failure of hydrodynamics in describing correctly the Poiseuille flow for dilute gases when the Knudsen number

exceeds 0.01, even when the gradients are relatively small. Deviations from hydro-
dynamics have been predicted since the development of kinetic theory [22] and per-
turbation techniques have been developed that allow the evaluation of corrections to
phenomenological laws of transport phenomena. When these corrections are inserted
into the general conservation equations, one obtains a set of partial differential equa-
tions for the hydrodynamic variables, commonly known as the Burnett equations [23].
The Burnett equations contain fourth- (or higher-) order spatial derivatives of hydro-
dynamic variables, thus requiring the specification of more boundary conditions than
those needed by the conventional fluid dynamic equations. So far, however, it is not
at all clear what form these additional boundary conditions must have. For this reason,
the Burnett equations have only been applied in specific situations where no bound-
ary conditions are required, as for example in problems dealing with strong shock
waves [24].

One alternative to the Burnett equations was recently proposed by Tij and
Santos [25]. They consider the Bhatnagar–Gross–Krook (BGK) approximation of the
Boltzmann equation [17,26] for the plane Poiseuille problem described in the previous
section. Using the symmetry properties of the flow, the BGK equation at the
stationary state takes the form,

$$\left(v_y \frac{\partial}{\partial Y} + a \frac{\partial}{\partial v_x} \right) f = - v(f - f_{LE}),$$ (6)

where f is the particle velocity distribution function, f_{LE} is the local equilibrium
distribution function,

$$f_{LE} = n(Y) \left(\frac{m}{2\pi k_B T(Y)} \right)^{3/2} \exp\left[-\frac{m}{2k_B T(Y)} (\mathbf{v} - \mathbf{u}(Y))^2 \right]$$ (7)

and v is the collision frequency,

$$v = 4nd^2 \sqrt{\frac{\pi k_B T}{m}} .$$ (8)

The boundary condition for (6) is $f(Y = \pm L/2) = f_R$ where f_R is the equilibrium
Maxwellian distribution at the reservoir temperature.

Despite its apparent simplicity, the BGK equation is extremely difficult to solve
explicitly, mainly because f_{LE} is a nonlinear functional of f through the hydrodynamic
variables $n(Y)$, $\mathbf{u}(Y)$ and $T(Y)$,[2]

$$\begin{pmatrix} n \\ n\mathbf{u} \\ 3nk_B T \end{pmatrix} = \int \begin{pmatrix} 1 \\ \mathbf{v} \\ m(\mathbf{v} - \mathbf{u})^2 \end{pmatrix} f(\mathbf{v}) \, d\mathbf{v} .$$ (9)

[2] Note that (9) defines the hydrodynamic variables as they are measured in the DSMC simulation. The integral
over f is approximated by the temporal and spatial average over particles located within a simulation volume
element (i.e., statistical samples are measured in a cell).

Suppose for a moment that the explicit form of these hydrodynamic variables was given. Eq. (6) could then be viewed as a non-homogeneous linear equation for f whose solution could be written as

$$f = (1 + \mathscr{L})f_{LE},$$ (10)

where $\mathscr{L}$ is a linear operator that incorporates the boundary conditions. In general, the explicit form of the hydrodynamic variables is not known a priori. Nevertheless, the solution (10) is still valid but it then represents only the *formal* solution of the BGK equation since f_{LE} remains a functional of f. The insertion of (10) into (9) leads to a closed set of five coupled nonlinear equations for the unknown functions $n(Y)$, $\mathbf{u}(Y)$ and $T(Y)$. Except for some very simple scenarios, these equations prove to be extremely difficult to solve [26]. Instead, Tij and Santos proposed to develop the formal solution (10) in powers of the external acceleration field a, looking for a "normal" solution of the BGK equation, where the spatial dependence of f is assumed to arise only through the hydrodynamic variables $n(Y)$, $\mathbf{u}(Y)$ and $T(Y)$. The calculations are tedious and lengthy, especially when the state dependence of the collision frequency v, Eq. (8), is taken into account. For this reason, we shall neglect the state dependence of v and simply discuss the final results (see [25] for details).

Define the scaled acceleration field as

$$\varepsilon \equiv \frac{amL}{2k_B T_R}.$$ (11)

The velocity profile reads

$$u_x(y) = \frac{avm}{2k_B T_R}L^2[(1/2)^2 - y^2][1 + O(\varepsilon^2)],$$ (12)

where we have set $y \equiv Y/L$. Noticing that the transport coefficients for the BGK model are

$$\eta_{BGK} = \frac{\rho k_B T}{vm}; \qquad \kappa_{BGK} = \frac{5k_B}{2m}\eta_{BGK}$$ (13)

then, to dominant order in ε, the relation (12) reduces to the hydrodynamic expression (1). However, a quantitative agreement with the simulations is obtained only if we use the correct Chapman–Enskog expression for the viscosity coefficient, Eq. (5), instead of the BGK result, Eq. (13) (see Fig. 4).

For the temperature profile, one finds

$$\frac{T(y)}{T_R} = 1 + 4\varepsilon^2 \left\{ \frac{v^2 m}{30k_B T_R}L^2[(1/2)^4 - y^4] - \frac{19}{25}[(1/2)^2 - y^2] \right\} + O(\varepsilon^4)$$ (14)

which is qualitatively different from the hydrodynamic profile (3), mainly because of the presence of an extra quadratic term (second term in the brace). Because of this term, the profile (14) exhibits a minimum at the center of the system, $y = 0$, and two maxima at

$$y_{\pm} = \pm\frac{1}{Lv}\sqrt{\frac{57k_B T_R}{5m}}.$$ (15)

Note that the separation of these maxima is proportional to the Knudsen number Kn, so they gradually merge at $y = 0$ as Kn is decreased. This is in qualitative agreement with the results of our simulations. The agreement, however, remains only qualitative and major quantitative discrepancies with the measured temperature profile are observed, even for a 40 mean free paths wide system.

One reason for this lack of quantitative agreement is that the transport coefficients obtained from the BGK model do not match those of hard spheres (cf. (5) and (13)). To account for this effect, we first observe that using the explicit form of transport coefficients for the BGK model, Eq. (13), the result (14), to dominant order in ε, can be written as

$$T(y) - T_R = \frac{a^2 \rho^2 L^4}{12 \eta_{BGK} \kappa_{BGK}} [(1/2)^4 - y^4] - \frac{19}{25} \frac{a^2 m^2 L^2}{k_B^2 T_R} [(1/2)^2 - y^2] . \tag{16}$$

The first term on the r.h.s. of (16) corresponds to the hydrodynamic profile (3). We can therefore replace η_{BGK} and κ_{BGK} in (16) by their correct hard sphere expressions, Eq. (5). Furthermore, in evaluating (16) we have neglected the temperature-dependence of the collision frequency, Eq. (8), which is evaluated at the reservoir temperature T_R. A better approximation is obtained by evaluating the r.h.s. of (16) at the average temperature in the system, T_{av}. These considerations lead to the following adjusted temperature profile,

$$T(y) - T_R = \frac{a^2 \rho^2 L^4}{12 \eta(T_{av}) \kappa(T_{av})} [(1/2)^4 - y^4] - \frac{19}{25} \frac{a^2 m^2 L^2}{k_B^2 T_{av}} [(1/2)^2 - y^2] . \tag{17}$$

Fig. 6 shows this adjusted profile together with the simulation results for a 10 mean free paths wide system. Again the temperature jump is chosen so as to match the measured profile in the middle of the system. Given the relatively large value of the expansion parameter, $\varepsilon = 0.3$, the agreement is fair, all the more so since the next order corrections to $T(y)$ turns out to be of the same order than the dominant term, Eq. (17). This, in turn, suggests that the expansion proposed by Tij and Santos is most probably asymptotic.

To obtain a more satisfactory agreement, we consider simulations with smaller values of ε. There exist several ways of lowering this parameter. One limitation is the desire to keep the flow sub-sonic since, otherwise, the shock waves generated in the system would make the theoretical interpretation of the results extremely difficult. On the other hand, the heat produced by the flow varies as the square of the velocity gradient so to have a nonequilibrium temperature profile that is measureable above the thermal noise of fluctuations, one needs to maintain the flow velocity as high as possible. From Eq. (1), the maximum value of the flow velocity is proportional to aL^2, so, to lower the value of ε, we have to increase the system size, while keeping the product aL^2 constant. Accordingly, we have considered a 20 mean free paths wide system containing 2000 particles, with $a = 4 \times 10^{-5}$. The results are depicted in Fig. 7, where excellent agreement with the theoretical predictions, Eq. (17), is now observed (see also Fig. 4).
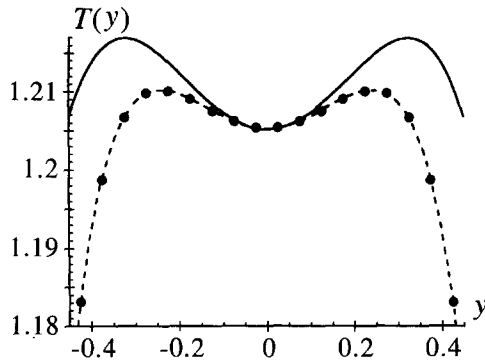
Fig. 6. Stationary temperature profile for a 10 mean free paths wide system; number density $n = 1.21 \times 10^{-3}$ and acceleration $a = 1.6 \times 10^{-4}$. The circles are simulation data and the solid line is from Eq. (17).
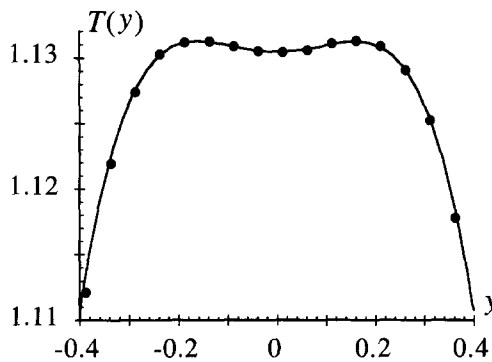

Fig. 7. Stationary temperature profile for a 20 mean free paths wide system; number density $n = 1.21 \times 10^{-3}$ and acceleration $a = 4.0 \times 10^{-5}$. The circles are simulation data and the solid line is from Eq. (17).

This result is rather surprising since the corresponding value of ε is only two times smaller than in the previous case, shown in Fig. 6. To check that this observed quantitative agreement is not due to a coincidence, we have also considered a 40 mean free paths wide system containing 4000 particles and setting the acceleration field to $a = 10^{-5}$. The results are depicted in Fig. 8, where the same excellent agreement is observed. These observations confirm further the asymptotic nature of the expansion of Tij and Santos. Note that in this last figure the kinetic theory prediction of the temperature jump, Eq. (4), was used with no additive adjustment of the profile so the agreement is completely quantitative.

We finally consider the pressure profile that, for the model used in this section, takes the following form:

$$\frac{P(y)}{P_R} = 1 - \frac{6}{5} \left(\frac{amL}{k_B T_{\mathrm{av}}} \right)^2 (1 - (y/L)^2) + O(\varepsilon^4), \tag{18}$$
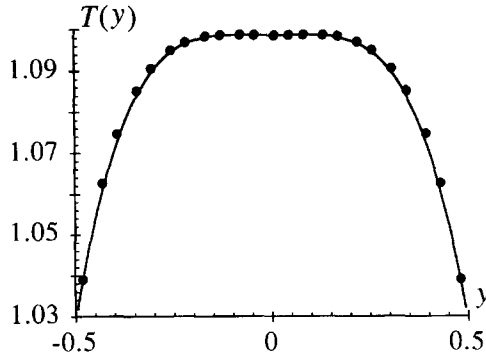
Fig. 8. Stationary temperature profile for a 40 mean free paths wide system; number density $n = 1.21 \times 10^{-3}$ and acceleration $a = 1.0 \times 10^{-5}$. The circles are simulation data and the solid line is from Eq. (17).
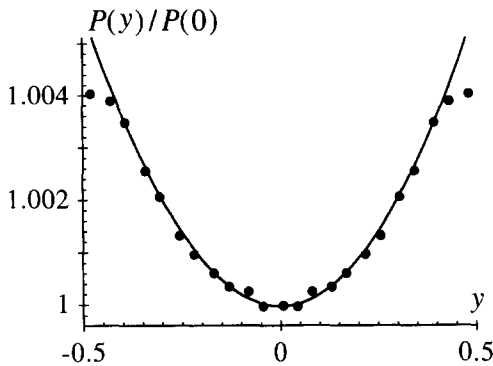

Fig. 9. Stationary pressure profile for a 40 mean free paths wide system; number density $n = 1.21 \times 10^{-3}$ and acceleration $a = 1.0 \times 10^{-5}$. The circles are simulation data and the solid line is the BGK first-order correction (see Eq. (18)). Both results are normalized by their corresponding values at the center of the system, $y = 0$.

where P_R is the pressure at the boundaries. A comparison of this result with the simulation data for a 10 mean free paths wide system was already presented in Fig. 3 where quantitative agreement is observed only near the origin, i.e., away from the boundaries. As we increase the system size, the agreement gradually improves, but the discrepancy remains observable near the boundaries even for a 40 mean free paths wide system (see Fig. 9). Full quantitative agreement is nevertheless observed for a 100 mean free paths wide system containing 10 000 particles, with $a = 1.6 \times 10^{-6}$ (see Fig. 5).

4. Concluding remarks

In this paper we have presented a detailed analysis of plane Poiseuille flow from three complementary points of view: microscopic simulations, macroscopic hydrodynamics

and kinetic theory. Discrepancies with the macroscopic hydrodynamic predictions were observed for Knudsen number as small as 0.01. Previous studies probably failed to notice these deviations since in many cases the relative differences are small. Thanks to DSMC's computational efficiency, we could measure the temperature and pressure profiles to high accuracy and establish that they differ structurally from hydrodynamic predictions. Regardless of how the equation of state, transport coefficients or boundary conditions are adjusted, the Navier–Stokes equations will never yield a bimodal temperature profile or a non-constant pressure profile.

The discovery of non-hydrodynamic behavior in a simple flow offers a good opportunity to test kinetic theory predictions. The profiles from the perturbative expansion of the BGK equation are shown to be in qualitative agreement with the simulation data. When the expansion parameter is small, quantitative agreement is obtained if the transport properties are suitably adjusted. Unfortunately, due to the complexity of the analysis, it is difficult to establish the specific reason why the hydrodynamic equations fail or if there exists an alternative macroscopic formulation that would give the correct profiles. Given the simplicity and symmetry of Poiseuille flow, an analysis using the Burnett equations appears promising. Work exploring this and other theoretical approaches is in progress.

Acknowledgements

References

[1] B.J. Alder, T.E. Wainwright, in: I. Prigogine (Ed.), Transport Processes in Statistical Mechanics, Interscience, New York, 1958; B.J. Alder, T.E. Wainwright, J. Chem. Phys. 31 (1959) 459; B.J. Alder, T.E. Wainwright, J. Chem. Phys. 33 (1960) 1439.

[2] B.J. Alder, T.E. Wainwright, Phys. Rev. A 1 (1970) 18; N.H. March, M.P. Tosi, Atomic Dynamics in Liquids, Dover, New York, 1976; S. Hess, C. Aust, L. Bennett, M. Kröger, C. Pereira Borgmeyer, T. Weider, Physica A 240 (1997) 126, these proceedings.

[3] W.G. Hoover, Computational Statistical Mechanics, Elsevier Sc. Publ., Amsterdam, 1991; D.J. Evans, G.P. Moriss, Eds., Statistical Mechanics of Non-equilibrium Liquids, Academic Press, New York, 1990.

[4] M. Mareschal, Ed., Microscopic Simulations of Complex Flows, Plenum, Nato ASI series, vol. 236, 1990; M. Mareschal, B. Holian, Eds., Microscopic Simulations of Complex Hydrodynamic Phenomena, Plenum, Nato ASI series, vol. 292, 1992.

[5] D.C. Rapaport, The Art of Molecular Dynamics Simulation, Cambridge University Press, Cambridge, 1995.

[6] D.C. Rapaport, E. Clementi, Phys. Rev. Lett. 57 (1987) 695; L. Hannon, G. Lie, E. Clementi, J. Sc. Comp. 1 (1986) 145; D.C. Rapaport, Phys. Rev. A 36 (1987) 3288; E. Meiburg, Phys. Fluids 29 (1986) 3107.

[7] M. Mareschal, E. Kestemont, Nature 323 (1987) 427; M. Mareschal, E. Kestemont, J. Stat. Phys. 48 (1987) 1187; D.C. Rapaport, Phys. Rev. Lett. 60 (1988) 2480.

[8] D.C. Rapaport, Phys. Rev. A 43 (1991) 7046; D.C. Rapaport, Phys. Rev. A 46 (1992) R6150.

[9] W.G. Hoover, Phys. Rev. Lett. 42 (1979) 1531; B.L. Holian, W.G. Hoover, B. Moran, G.K. Straub, Phys. Rev. A 22 (1980) 2798; B.L. Holian, Phys. Rev. A 37 (1988) 2562.

[10] M. Mareschal, M. Malek Mansour, A. Puhl, E. Kestemont, Phys. Rev. Lett. 61 (1988) 2550; A. Puhl, M. Malek Mansour, M. Mareschal, Phys. Rev. A 40 (1989) 1999.

[11] J. Koplik, J.R. Banavar, Annu. Rev. Fluid Mech. 27 (1995) 257.

[12] J.C. Maxwell, Philos. Trans. London 70 (1867) 231.

[13] J. Koplik, J.R. Banavar, J.F. Willemsen, Phys. Fluids A 1 (1989) 781; D.L. Morris, L. Hannon, A.L. Garcia, Phys. Rev. A 46 (1992) 5279.

[14] D.C. Wadsworth, Phys. Fluids A 5 (1993) 1831.

[15] M. Malek Mansour, F. Baras, Physica A 188 (1992) 253.

[16] L.D. Landau, E.M. Lifshitz, Fluid Mechanics, Pergamon, Oxford, 1959.

[17] C. Cercignani, The Boltzmann Equation and its Applications, Springer, New York, 1988; C. Cercignani, Mathematical Methods in Kinetic Theory, Plenum, New York, 1990.

[18] G.N. Patterson, Molecular Flow of Gases, Wiley, New York, 1956; V.P. Shidlovskii, Introduction to Dynamics of Rarefied Gases, Elsevier, New York, 1967.

[19] E.H. Kennard, Kinetic Theory of Gases, McGraw-Hill, New York, 1938; D.K. Bhattacharya, G.C. Lie, Phys. Rev. Lett. 62 (1989) 897.

[20] G.A. Bird, Molecular Gas Dynamics, Clarendon, Oxford, 1976; G.A. Bird, Molecular Gas Dynamics and the Direct Simulation of Gas Flows, Clarendon, Oxford, 1994.

[21] L. Hannon, G. Lie, E. Clementi, Phys. Lett. A 119 (1986) 174.

[22] S. Chapman, T.G. Cowling, The Mathematical Theory of Non-Uniform Gases, Cambridge University Press, Cambridge, 1960.

[23] J.H. Ferziger, H.G. Kapper, Mathematical Theory of Transport Processes in Gases, North-Holland, Amsterdam, 1972.

[24] E. Salomons, M. Mareschal, Phys. Rev. Lett. 69 (1992) 269.

[25] M. Tij, A. Santos, J. Stat. Phys. 76 (1994) 1399.

[26] A. Santos, J.J. Brey, C.S. Kim, J.W. Dufty, Phys. Rev. A 39 (1989) 320; C.S. Kim, J.W. Dufty, A. Santos, J.J. Brey, Phys. Rev. A 40 (1989) 7165.